Robotica (2011) volume 29, pp. 595–605. © Cambridge University Press 2010
doi:10.1017/S0263574710000408

Energy-efficient gait generation for biped robot based on the passive inverted pendulum model

Jian Li and Weidong Chen*

Department of Automation, Shanghai Jiao Tong University, Shanghai 200240, P.R. China

(Received in Final Form: July 16, 2010. First published online: August 19, 2010)

SUMMARY

From the viewpoint of the system's mechanical energy, the passive inverted pendulum model (PIPM) is proposed for the generation of more energy-efficient biped gait pattern. The generated walking pattern, based on the PIPM, enables the fully actuated biped robots to closely mimic the behavior of stable passive walking, so that it can have good energy-efficiency, which is the inherent advantage of the passive system. Furthermore, the pattern generation method is extended to any desired terrain as well. As for SHR-1, the first-generation biped robot of Shanghai Jiao Tong University, gait synthesis is clarified in detail. Finally, the walking experiments are carried out on SHR-1, and the effectiveness of the proposed pattern generation method is confirmed.

KEYWORDS: Biped robot; Walking pattern generation; Dynamic walking; PIPM.

1. Introduction

Biped humanoid robots have become one of the most challenging researches of the intelligent robots in the past two decades. Many biped humanoid robots have been developed, such as Asimo,[1] HRP,[2] WABIAN,[3] KHR,[4] and Johnnie,[5] where various types of dynamic walking can be performed. However, there remains a central problem to be dealt for most of these biped robots: it is difficult to utilize robot inherent dynamics for realizing natural and energy-efficient walking, which limits the robot practicable application due to the limitation of the energy supply. Generally, there exist two major approaches for improving energy efficiency for the biped locomotion.

The first approach aims at reducing the energy consumption by improving the conventional gaits with more human-like walking patterns. For most conventional robots that can walk stably, the walking motion patterns of most robots are obviously different from that of human beings: a human being utilizes up-and-down motion of the upper body to walk efficiently, while these conventional humanoid robots keep the height of the hip constant.[2–9] Though keeping the height of the hip constant hardly affects the position of the zero moment point (ZMP), the generated motion patterns are neither human-like nor energy-efficient. Therefore, some researchers put forward their methods. Taking "straight legged walking" as design objective, Yu *et al.*[10,11] predetermined the knee trajectories as one of the initial walking parameters to solve the waist trajectory based on ZMP criterion. Kurazume *et al.*[12] realized the straight legged walking by controlling the height of the center of gravity (COG) trajectory according to the state of the ZMP controller. Sekiguchi *et al.*[13] directly added the up-and-down motion of the waist to the COG motion generated by the linear inverted pendulum model (LIPM) in the horizontal direction to obtain more natural biped walking. Although these methods can realize more human-like waking pattern, whether the gaits they achieve are energy-efficient than conventional pattern is open to discussion.

The second approach is established upon passive dynamics of the biped system. McGeer's passive–dynamic walker[14,15] exhibited remarkably human-like walking motions on a shallow slope though it had no actuators or controllers, which showed the principle for natural and efficient walking by utilizing the dynamical property of the walker. Collins *et al.*[16,17] presented three robots based on passive dynamics with small active power sources. Anderson *et al.*[18] described the design and the control of the three biped robots which were based on passive dynamic. Asano *et al.*[19] proposed energy-constraint control for the walking of a planar robot without any gait planning and design in advance. Without regard of the biped motion in the lateral plane, Westervelt *et al.*[20] developed virtual constraints and hybrid zero dynamics for controlling a five-link biped called RABBIT from a hybrid system point of view. These robots have augmented the passive dynamics with actively power and they can acquire asymptotically stable, high energy-efficient and startling human-like locomotion, but thus far have demonstrated poor versatility and robustness because of underactuation, which enables the passive dynamics. Today, the researchers are striving for acquiring better versatility and robustness by gradually adding active power to the underactuated robots with maintaining high energy-efficiency of the passive robots.

Practical biped robots need to be versatile, robust, and energy-efficient. Based on the above analysis, in this paper, we reconsider the gait generation mechanism for the fully-actuated biped robots from the viewpoint of the system's mechanical energy. We derive the passive inverted pendulum model (PIPM), which reflects the principle relation between the system's energy change and its COG. The main goal is to transfer the desirable properties of passive walking to fully actuated biped robots in order to inherit the good energy-efficiency, which is the inherent advantage of the passive

* Corresponding author. E-mail: wdchen@sjtu.edu.cn

system. The PIPM is derived by imposing the "Zero-State" constraint on the inverted pendulum model of the biped robot. The "Zero-State" constraint is introduced based on the motion analysis of the passive–dynamic walking form the viewpoint of energy. For the biped walking using the generated pattern based on the PIPM, the COG begins to move under the gravity while its potential energy is being translated to the kinetic energy, and the kinetic energy of forward motion starts to be traded for a rise in potential energy by the switching of the supporting leg. Since the proposed pattern maintains continuous gait cycle by means of the energy conversion, it is energy-efficient and exhibits up-and-down motion of the upper body. In addition, the walking pattern generation on the flat and any desired terrain are clarified in this paper.

The rest of the paper is organized as follows: Section 2 presents the PIPM and describes the way how to use the PIPM to generate walking pattern on the flat ground. In Section 3, the pattern generation method is extended to any desired terrain. Section 4 introduces the prototype biped robot SHR-1 and clarifies the gait synthesis. In Section 5, the comparison of the proposed walking pattern with the conventional pattern shows the advantage of the proposed walking pattern, and the walking experimental results carried out on SHR-1 is also provided. Finally, the conclusion is given in Section 6.

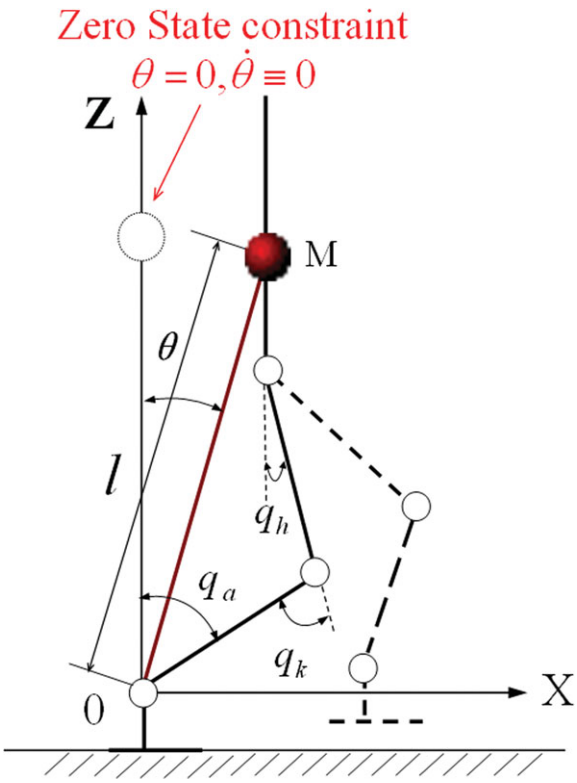

Fig. 1. Five-link passive inverted pendulum model (origin of coordinates lies in ankle of the supporting foot).

2. Pattern Generation Based on PIPM

For a five-link biped model, it has been noticed that the joint angle profiles can be determined if compatible trajectories for the COG and the tip of the swing leg can be prescribed. In this section, emphasis is placed on the trajectory generation of the COG, and then a step cycle is arranged to take the double support phase (DSP) into consider.

2.1. Passive inverted pendulum model

When a biped robot is supporting its body on one leg, its dominant dynamics can be represented by a single inverted pendulum with stationary pivot point, which is composed of a point-mass denoted by M and a massless rod with the length l, as shown in Fig. 1. In this paper, the PIPM is used to describe the free falling motion of the inverted pendulum, which means that it begins to accelerate away from the vertical stationary state thanks to gravity.

The passive–dynamic walkers can walk down a shallow slope with startlingly human-like gait though they have no actuation or control. This is due to the energy conversion between the kinetic energy and the potential energy, and the change of the gravitational potential energy owing to the slope is in charge of compensating the energy loss caused by the repetitive impacts of the swing leg with the ground at the heel strike. Take no account of energy losses, the mechanical energy E of the robot is defined as

$$E(q, \dot{q}) = \frac{1}{2}\dot{q}^T M(q)\dot{q} + P(q) \equiv P_{\max},$$

where $M(q)$ is the inertia matrix, $P(q)$ is the potential energy with the tip of the stance leg as a standard, q is the vector of joint angles, $P_{\max}$ is the maximum potential energy when the passive–dynamic walker begins to move from the stationary time ideally ($q = 0, \dot{q} = 0$). In terms of the PIPM, the potential energy is the maximum when it stands upright. According to characteristic of the passive–dynamic walking, the robot keeps stationary when it reaches the maximum potential energy. Therefore, we call the stationary upright state as "Zero-State."

In order to make the biped robot to walk like a passive–dynamic walker, the PIPM is derived on the basis of two assumptions and one "Zero-State" constraint. The two assumptions are made as follows:

(1) The contact between a robot and the surface is point-contact.
(2) The robot motions in sagittal and lateral planes are independent.

The point-contact assumption means that the ankle joint of the supporting foot is passive. Namely, the surface has no influence on the robot dynamics and there is zero torque between the ankle joint and the surface, which makes it possible to control the robot based on its inherent dynamics. The second assumption enables the biped walking motions in the sagittal and lateral planes to be treated separately. Though the motions in the sagittal and lateral planes couple with each other in the Z-axis direction, their maximum displacements are 1.58 cm and 0.82 cm, respectively, in the Z-axis direction when the robot walks with step length of 25 cm. Comparing with the height of COG (about 48.5 cm with our robot), the Sagittal and lateral planes have little kinematics and dynamics effects on the other plane. Therefore it is acceptable that the sagittal and lateral motions are assumed to

https://doi.org/10.1017/S0263574710000408 Published online by Cambridge University Press

be decoupled. Constrained with the "Zero-State" constraint, the PIPM model will satisfy the ZMP concept, which means the motion of it can keep stable.

The motion of the PIPM in the sagittal and lateral planes can be given as

$$\ddot{\theta} = \frac{g}{l}\sin\theta, \tag{1}$$

$$\ddot{\phi} = \frac{g}{l}\sin\phi, \tag{2}$$

$$\dot{\theta} \equiv 0, \quad when\ \theta = 0, \tag{3}$$

where θ and ϕ are the pendulum angles in the sagittal and lateral planes respectively, and g is the acceleration of gravity. In the following section, the way how to generate the trajectory of the COG by the proposed PIPM is introduced in detail.

2.2. *Trajectory of the COG*

In the sagittal plane, let (x_C, z_C) be the position of the COG and the origin of the local coordinates system lie in the ankle of the supporting foot, as depicted in Fig. 1, then the position of COG can be depicted as below:

$$\begin{cases} x_C = l\sin\theta, \\ z_C = l\cos\theta. \end{cases} \tag{4}$$

For bipedal locomotion, it is desirable for the biped robot to move steadily, which means the cyclic biped walking pattern is required to be continuous and repeatable. Supposing that the time period for one walking step is T_S, then the time of the kth step walking begins at the time (kT_S) when the swing leg hits the ground and ends at the time $((k+1)T_S)$ when the other leg becomes the swing leg and hits the ground. According to the periodicity and the symmetry of the gait,[8] there exists the following constraints:

$$\begin{cases} x_C((k+1)T_S) - x_C(kT_S) = S_S, \\ z_C((k+1)T_S) = z_C(kT_S), \end{cases} \tag{5}$$

where S_S is the step length.

Assuming that the time when the COG passes the normal axis is t_1, the imposed "Zero-State" constraint can be expressed as

$$\begin{cases} \theta(t_1) = \theta(kT_S + t_1) = 0, \\ \dot{\theta}(t_1) = \dot{\theta}(kT_S + t_1) = 0. \end{cases} \tag{6}$$

For a general walking (the length of a stride does not change during the period of the walking), the switching of the gait happens at the intermediate point of a stride, which means t_1 equals to $T_s/2$. So the following relations from the repeatability and the continuity of the gait can be derived as

$$\begin{cases} \theta((k+1)T_S) = -\theta(kT_S) = \arcsin\left(\dfrac{S_S}{l}\right), \\ \theta\left(kT_S + \dfrac{T_S}{2}\right) = 0. \end{cases} \tag{7}$$

According to the constraints (5), (6), and (7) for the COG, the solution for Eq. (1) can be expressed as follows:

$$\theta(t) = K_q(e^{Kt} - e^{-Kt}) \tag{8}$$

$$\text{where } K = \sqrt{\frac{g}{l}},\ K_q = \frac{\arcsin\left(\dfrac{S_S}{l}\right)}{\left(e^{\frac{-KTs}{2}} - e^{\frac{KTs}{2}}\right)}.$$

Equation (8) indicates that trajectory of the COG motion of a biped robot is determined by the walking pattern parameters uniquely in the sagittal plane.

The trajectory of the COG in the lateral plane is derived by adopting the similar method. The major constraint equations are listed as follows:

$$\begin{cases} \phi(kT_S) = \phi((k+1)T_S) = \arcsin\left(\dfrac{A_y}{l}\right), \\ \phi\left(kT_S + \dfrac{T_S}{2}\right) = \dot{\phi}\left(kT_S + \dfrac{T_S}{2}\right) = 0, \end{cases} \tag{9}$$

where A_y is the lateral swing amplitude of the COG in a step cycle.

2.3. *Step walking cycle arrangement*

In this paper, a step walking cycle is specified that begins with a DSP and ends with a single support phase (SSP). The DSP is the period when both feet of the robot are in contact with the ground. The DSP plays an important role in achieving smoothly stable walking when the COG is moved from one leg to the other. According to human beings, the DSP takes about over 10% of the period of one step walking,[21] and it is specified eighth of a step walking cycle in this paper.

The COG begins with the trajectories derived from the PIPM in the sagittal and lateral planes simultaneously in the DSP, and the swing leg begins to move when the DSP ends. We can specify the trajectory of the swing leg tip by means of a spline function according to the repeatability and the continuity of the gait and the ground condition.

From the viewpoint of natural human walking, it is desirable that the upper body is kept directly upward or oscillates slightly around the upright position.[22] For a five-link biped model as shown in Fig. 1, the joint angle profiles can be determined if compatible trajectories for the hip and the tip of the swing leg can be prescribed, all the joint trajectories of the biped robot will be determined by its kinematics constraints, and the walking pattern can be denoted uniquely.

3. Pattern Generation Extended to Any Desired Terrain

For a lumped-mass model, when the external force does not act to the biped robot, the ZMP can be calculated by

$$x_{ZMP} = x_C - \frac{\ddot{x}_C z_C}{\ddot{z}_C + g}, \tag{10}$$

$$y_{ZMP} = y_C - \frac{\ddot{y}_C z_C}{\ddot{z}_C + g}. \tag{11}$$

https://doi.org/10.1017/S0263574710000408 Published online by Cambridge University Press

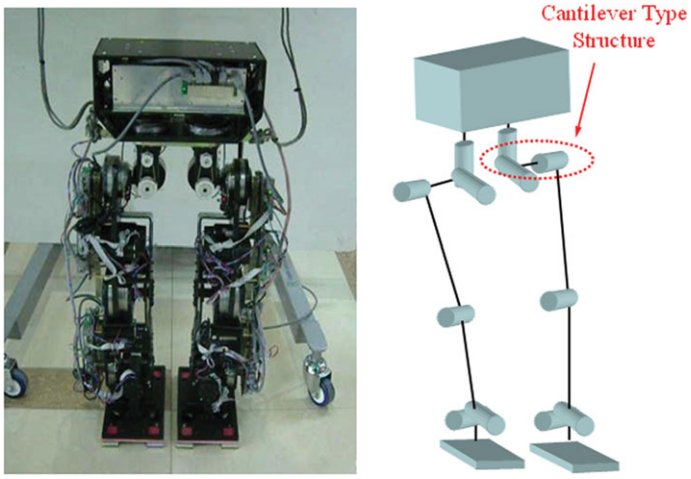

Fig. 2. Photograph and joint arrangement of SHR-1.

In the local coordinate system as depicted in Fig. 2, for the PIPM, the ZMP is kept as ($x_{ZMP} \equiv 0$, $y_{ZMP} \equiv 0$) according to the definition of the ZMP.[6] From Eqs. (10) and (11), we can see that COG motions in the sagittal and lateral planes can not be specified arbitrarily. In the sagittal plane, we can define the COG motion as

$$z_C = f(x_C) + s(t), \tag{12}$$

where $z_C = f(x_C)$ stands for the COG motion of a PIPM in the sagittal plane, and $s(t)$ contains the additional motion of the COG in the Z direction besides the motion of the PIPM. So we can derive the following equations:

$$x'_{ZMP} = x_C - \frac{\ddot{x}_C f(x_C)}{\ddot{f}(x_C) + g} = 0, \tag{13}$$

$$x_{ZMP} = x_C - \frac{\ddot{x}_C (f(x_C) + s(t))}{(\ddot{f}(x_C) + \ddot{s}(t)) + g} = 0. \tag{14}$$

From Eqs. (13), (14), and (15), we can derive

$$\frac{\ddot{s}(t)}{s(t)} = \frac{\ddot{x}_C}{x_C}. \tag{15}$$

The trajectory of COG in the sagittal plane has been derived from the PIPM. Furthermore, we can derive the constraints of $s(t)$ due to the periodicity and symmetry of the gait as

$$\dot{s}(kT_s) = \dot{s}((k+1)T_s) = 0. \tag{16}$$

According to the ground geometric condition as well as the Eqs. (15) and (16), we can derive the trajectory of COG in the sagittal plane for any known ground. Combined the trajectory of the COG with the trajectory of the tip of swing leg on the corresponding ground, the walking pattern can be acquired. Note that the method introduced above does not concern the change of the gait parameters (step length, step height, and etc.) due to the geometric constraint of the landing area, which means the swing foot has to land on a continuous region near the landing foot on the ground. The applications of this method include the walking surfaces such as slope surface, stairs, etc.

4. Gait Synthesis of Biped Robot SHR-1

4.1. Biped robot SHR-1

Figure 2 shows the biped robot SHR-1, which has been developed since 2006. Because our main purpose to study the biped walking, the upper body of SHR-1 is ignored and the power supply is provided outside. Its total weight is 32 kg and its height is 85 cm, and the overall height of SHR-1 with body and head is designed to be about 130 cm. SHR-1 has 6 DOFs in each leg, where 3 DOFs are for the hip, 1 DOF is for the knee and 2 DOFs are for the ankle. The hip joint of SHR-1 has a cantilever type structure as HRP,[2] which is designed for some special motions such as the catwalk, in that the cantilever type structure hip enables to have less collision between inside upper-limbs of the legs. In addition, most mechanical parts of SHR-1 are made of aluminum except that the hip mechanical structure is made of titanium alloy. This is due to the fact that the hip joint tends to suffer great mechanism deformation during walking. The hip joints and ankle joint are designed to cross at one point separately, as shown in Fig. 1. The axes intersection design leads to less computation complexity of coordinate transformation in the forward kinematics and inverse kinematics calculation. All the joints of SHR-1 are actuated by DC motors and harmonic drive reduction gears with pulley-belts used as main reduction gears. The motors and reduction gears are selected based on the simulation results where some special motions are simulated. The total reduction ratios of reduction gears and pulley-belts are chose to balance the speed and the torque of the joints. The overall specifications of SHR-1 are given in Table I.

Distributed control system architecture is adopted in SHR-1. The main computer is embedded in the biped robot, and

Table I. Specification of SHR-1.

Biped Robot		SHR-1
Dimensions	Height	85.0 cm
	Upper leg length	23.5 cm
	Lower leg length	23.5 cm
	Ankle-sole height	10.8 cm
	Length between hip joints	12.0 cm
	Toe-heel length	2.2 cm
Weight	32 kg	
D.O.F	12 D.O.F	
Walking speed	Up to 1.2 km/h	
Actuator	Servo DC + harmonic drive gear + pulley-belt	
Sensors	Torso	Rate gyro/acceleration sensor
	Foot	3-axis Force/torque sensor
	Joint	Position sensor
Operating system	RT-Linux	

https://doi.org/10.1017/S0263574710000408 Published online by Cambridge University Press

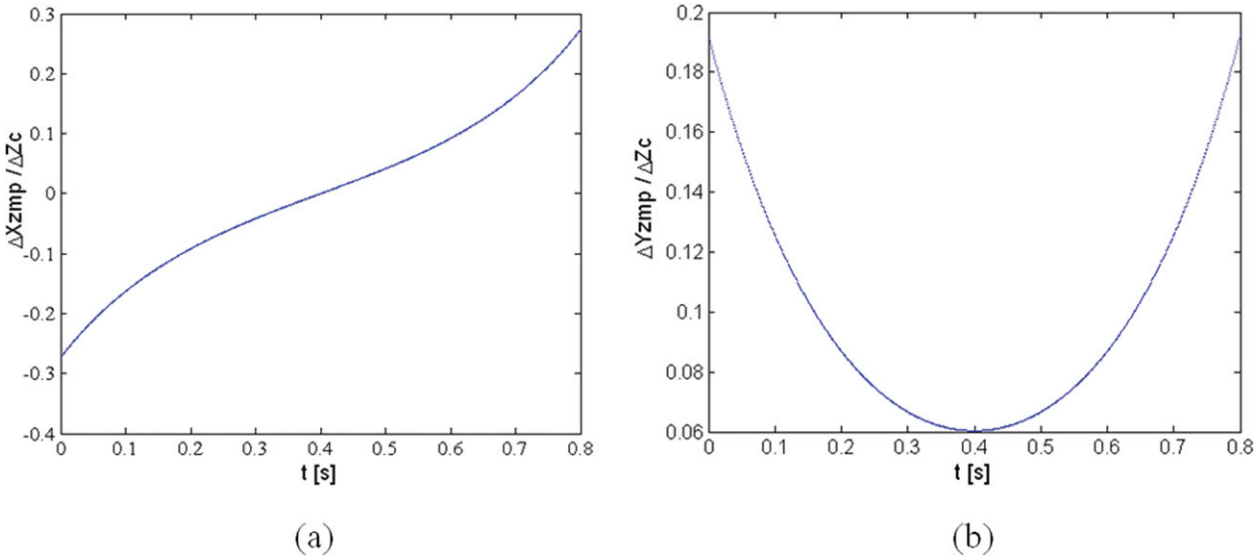

Fig. 3. Effects of the COG's height deviation on the stability during one step cycle, where (a) ZMP deviation in the sagittal plane, (b) ZMP deviation in the lateral plane.

it connects 12 subcontrollers, one inertial sensor and two six-axis Force/torque sensors with CAN communication. With RT-Linux real-time operation system (OS), the robot is controlled with about 150 Hz control frequency, which are necessary for the control of the biped walking.

4.2. Determination of the PIPM parameters according to SHR-1

To apply the PIPM to generate the gait pattern of SHR-1, the key is the determination of the pendulum length connecting the COG with the ankle of the supporting leg (l), which represents the distance between the COG and the ankle of the supporting leg.

Let Δz_C represent the deviation of COG's height, $(\Delta x_{ZMP}, \Delta y_{ZMP})$ represent the ZMP deviation. The following equation can be derived based on ZMP equation (10):

$$(x_{ZMP} + \Delta x_{ZMP}) = x_C - \frac{\ddot{x}_C(z_C + \Delta z_C)}{(z_C + \Delta z_C)'' + g}. \tag{17}$$

For the deviation of COG's height $\Delta z_C \ll z_C, (z_C + \Delta z_C)'' \approx \ddot{z}_C$ can be obtained. Therefore, the following equation can be concluded from the Eq. (17):

$$\frac{\Delta x_{ZMP}}{\Delta z_C} = \frac{\ddot{x}_C}{\ddot{z}_C + g}. \tag{18}$$

Equation (18) is the ZMP deviation due to the deviation of COG's height in the sagittal plane, the ZMP deviation in the lateral plane can be derived according to the above method. Figure 3 shows the ZMP deviation due to the deviation of COG's height during one step cycle. It is seen that the height of COG has great effects on the stability of the biped walking. For SHR-1, the stability range is defined as $-8\,\text{cm} \le x_{ZMP} \le 8\,\text{cm}$ and $-4\,\text{cm} \le y_{ZMP} \le 4\,\text{cm}$ due to the dimension of its feet ($20\,\text{cm} \times 12\,\text{cm}$). Therefore, it is expected that the pendulum length could approach the real COG's height as accurately as possible, so that the robot can have best stability. Though the COG's height can be calculated roughly, but the accurate value is hard to acquire according to the complex structure of the biped robot. Finally, the pendulum length is determined as 48.5 cm experimentally by making the robot to have the best stability.

The walking motion of the robot in the sagittal plane is determined by the gait parameters including the step length S_s, the step period T_s and the maximum step clearance H_s. The lateral swing amplitude of the waist A_y is the major parameter for the biped walking motion in the lateral plane. Theoretically, its value can be chosen as half of the distance between the two feet at the initial home posture, which is 9 cm. For SHR-1, it becomes larger due to the fact that the robot's absence of the upper body and the value for it is 9.5 cm.

5. Walking Simulation and Experiments

In this section, two kinds of gait generation for a biped robot are demonstrated. By using the detailed model of the biped robot SHR-1, the proposed pattern generation can be verified.

5.1. Comparison of a conventional pattern with the proposed pattern

Figure 4 shows the comparison of a conventional walking pattern with a constant waist height and the proposed walking pattern. The dashed line is for the walking during the DSP, while the solid line is for the walking during the SSP. Both of the two walking patterns have the same gait parameters: step length of 25 cm, step period of 1.6 s, and step height of 2 cm, the model parameters are determined based on biped robot SHR-1. In the comparison graph, the marks "*" represent the position of COG, and it can be seen that the proposed walking pattern reveals an up-and-down motion of the COG, which is one of the characteristics of human walking. However, the walking motion of conventional pattern is not as natural as those humans by keeping a constant waist height at about 48 cm. Moreover, the COG motion of the proposed walking pattern does not keep constant

https://doi.org/10.1017/S0263574710000408 Published online by Cambridge University Press

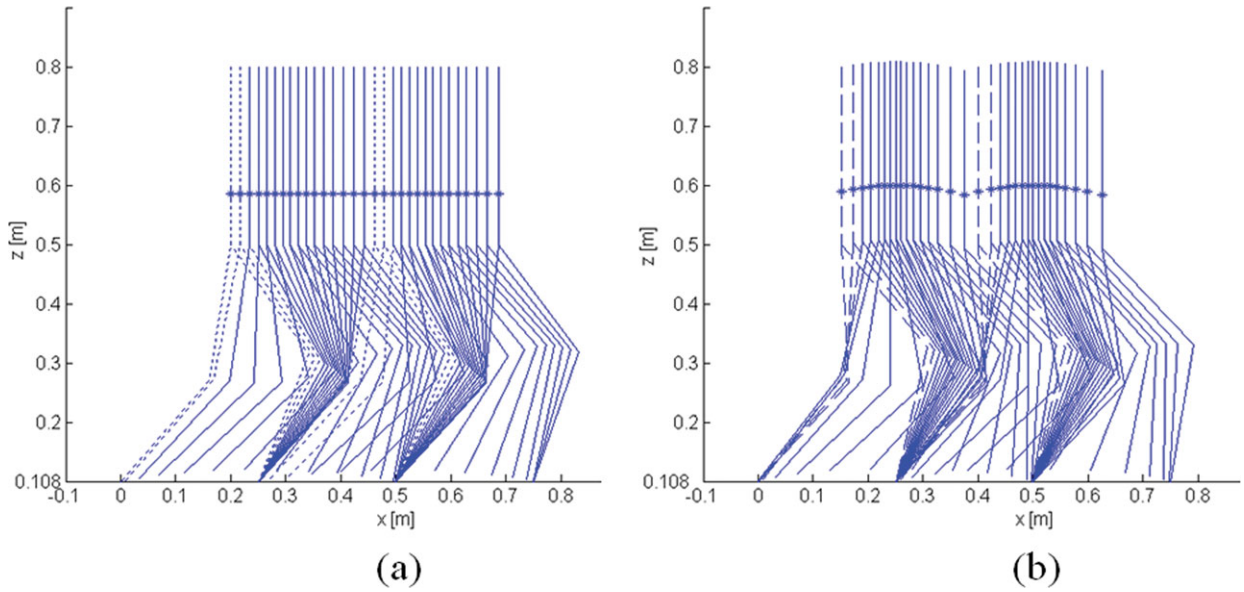

Fig. 4. Stick diagrams of the five-link biped, where (a) conventional walking pattern, (b) proposed walking pattern.

velocity in the moving direction, which can be seen from the human walking and the compass-gait of the passive–dynamic walkers.

Figure 5 shows the calculated joint torque at the knee joint of the right leg in three walking cycle. Figure 6 shows the total power consumption in three walking cycle. It can be seen that the proposed walking pattern is more efficient than the conventional walking pattern with a constant waist height. In addition, the specific resistance is computed for comparing efficiency with other robots of different sizes, defined as $\varepsilon =$ (energy used)/(weight $\times$ distance traveled), which means the expenditure of energy per unit mass and per unit distance traveled.[16] For the walking experiments of SHR-1 with step length of 0.25 m, step period of 1.6 s/step and step height of 0.02 m, the specific resistance with the conventional pattern was 2.87, while the value was 1.80 with the proposed pattern. The specific resistance was improved approximately by 37.3%.

5.2. *Biped walking on the flat ground*

The gait parameters of the proposed walking pattern on the flat ground are represented in Table II, and the geometrical parameters for inverse kinematics calculation to derive the joint angles of SHR-1 are the dimensions of Table II.

Figure 7 shows the motion of the COG for the walking on the flat ground. In the middle of a step period, the height

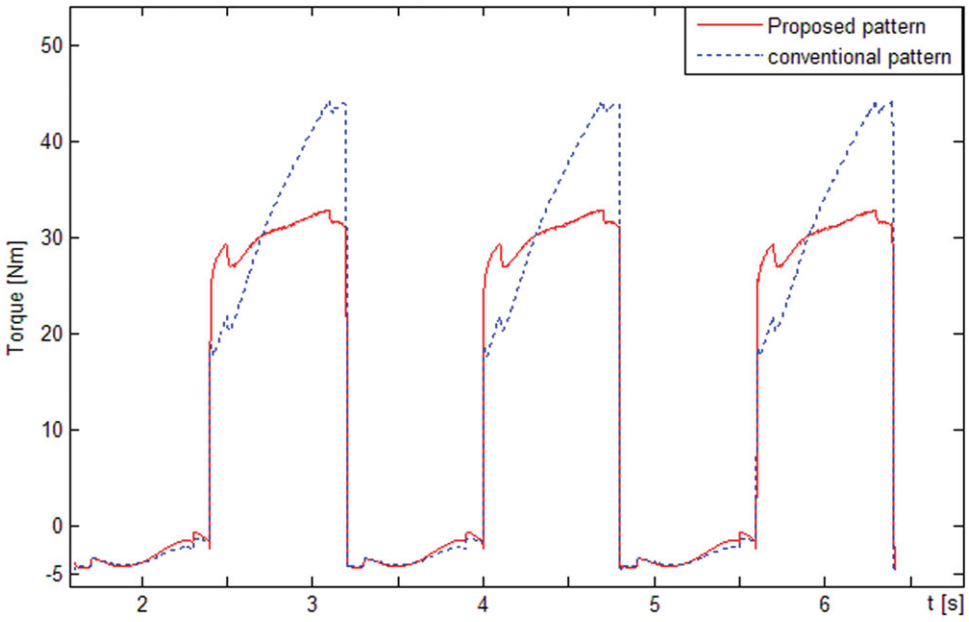

Fig. 5. Torque at knee joint of the right leg.

https://doi.org/10.1017/S0263574710000408 Published online by Cambridge University Press

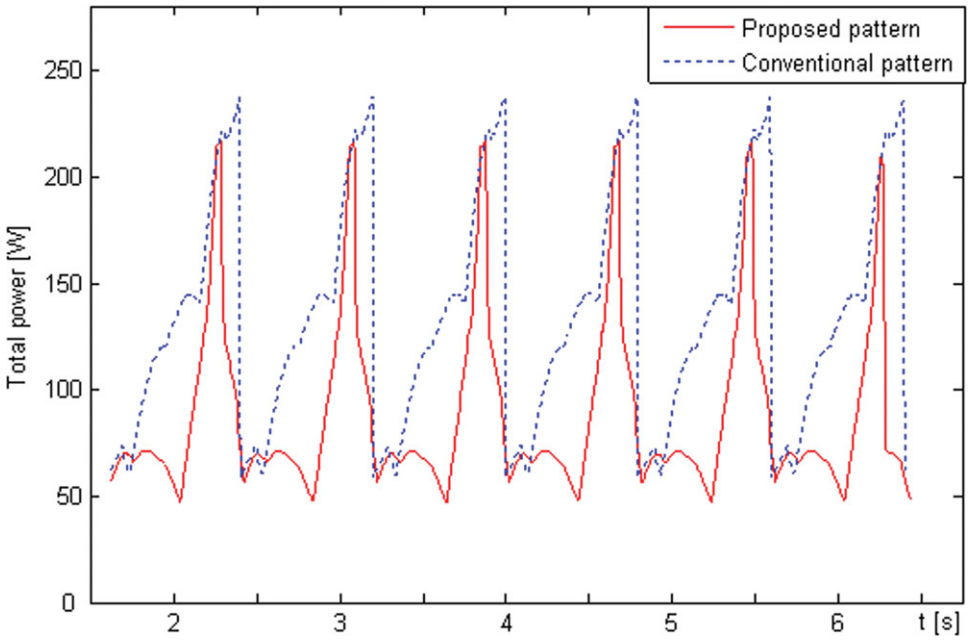

Fig. 6. Total power consumption.

Table II. Gait parameters of walking on the plat ground.

Gait parameters		Value
Step length (stride/2)	S_s	0.25 m
Lateral swing amplitude of pelvis	A_y	0.09 m
Maximum step clearance	H_s	0.02 m
Step period	T_s	0.8 s
DSP	T_d	0.1 s
SSP	T_{sp}	0.7 s

Table III. Gait parameters of walking on the slope.

Gait parameters		Value
Slope angle		3°
Step length (stride/2)	S_s	0.2 m
Lateral swing amplitude of pelvis	A_y	0.09 m
Maximum step clearance	H_s	0.02 m
Step period	T_s	1.6 s
Single support period	T_{sp}	1.4 s
Double support period	T_d	0.2 s

of the COG reaches peak, and the robot have the maximum potential energy. When the role of the supporting leg becomes to change, the robot has the maximum kinetic energy to help the role change. This is similar to that in the walking pattern of the passive–dynamic walkers.

Figure 8 shows the joint angles of one leg for the generated walking pattern in the sagittal plane. The walking gait is divided into the SSP, the DSP, and the swing leg phase (SLP). It is seen that the joint angles is continuous and smooth during the SSP and the DSP. What is more, the proposed walking pattern is human-like: the knee joint of the supporting leg almost keeps motionless during the SSP while the body is rotating around the ankle of the supporting leg, and the knee joint moves to lift the swing leg from the ground during the SLP. Because the knee joint of the supporting leg suffers the maximum torque, keeping motionless is helpful to reduce the energy cost of the biped during walking.

Figure 9 shows the snapshots of the biped walking on the concrete flat ground. Though the ground is a little uneven, the robot can remain a good stability.

5.3. Biped walking on the slope

With known angle of the slope, we can determine the trajectory of COG using the pattern generation method in Section 3. The gait parameters of the proposed walking pattern on the slope are represented in Table III, and the geometrical parameters for inverse kinematics calculation to derive the joint angles of SHR-1 are the dimensions of Table I.

Figure 10 shows the height of the COG when the robot walks on the slope with the proposed pattern generation. The cyclic height of the COG is raised to adapt to the geometrical constraint of the slope.

Figure 11 shows the snapshots of the biped walking on the slope. In the beginning, the distance between the biped robot and the slope is known. It can be seen that the robot can walk stably onto the slope.

6. Conclusions and Future Work

In this paper, a new model named Passive Inverted Pendulum (PIPM) is proposed for generating walking pattern for a fully actuated biped robot. The PIPM is derived from the viewpoint of the biped system's energy conversion inspired by the passive–dynamic walking. The walking pattern based on the PIPM has the following advantages: (1) human-like natural waking pattern is obtained which

https://doi.org/10.1017/S0263574710000408 Published online by Cambridge University Press

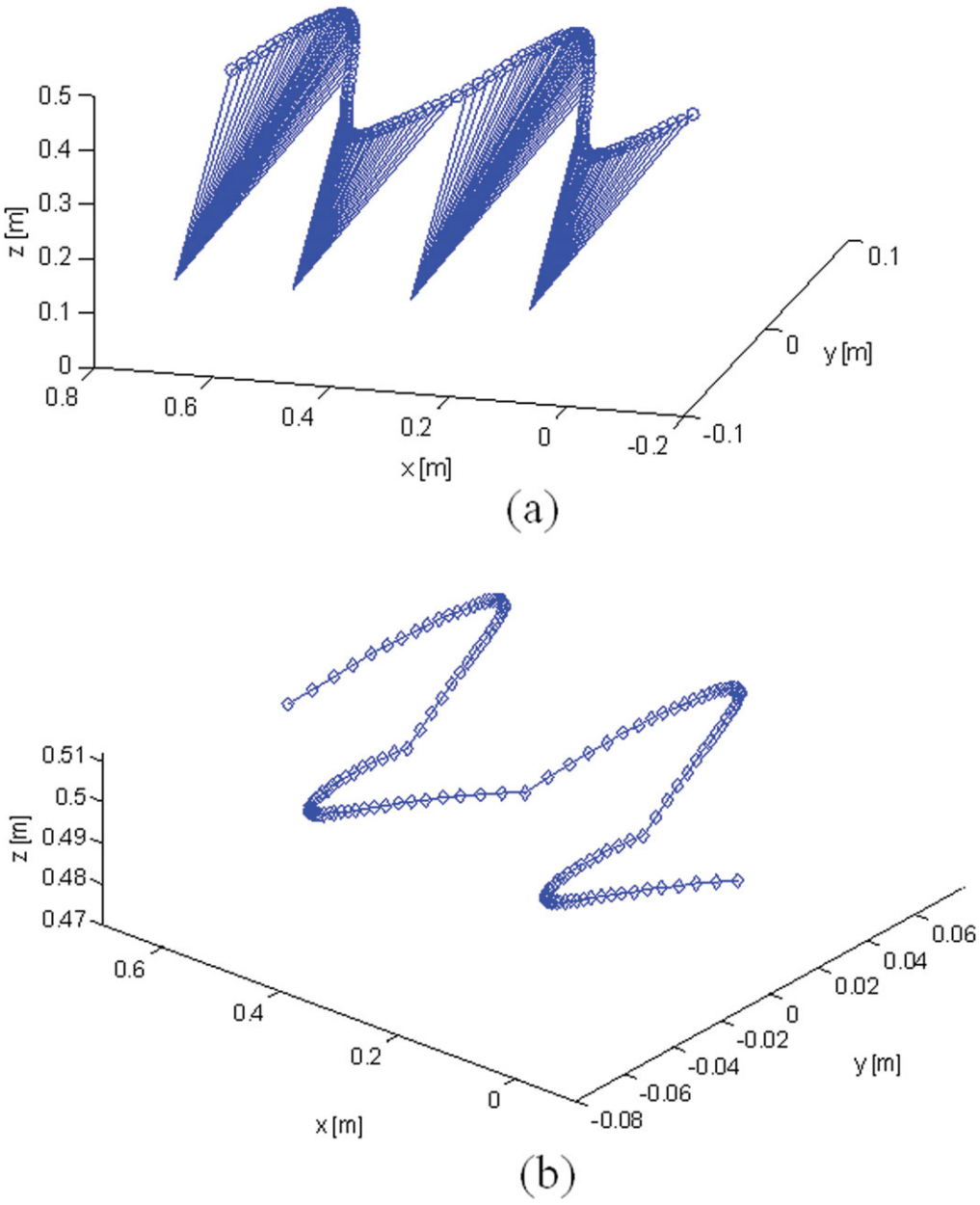

Fig. 7. Three-dimensional walking pattern, where (a) COG motion relative to the supporting point, (b) COG motion in 3D plane.

utilizes up-and-down motion of the upper body; (2) in terms of specific resistance, the energy-efficiency of the proposed walking pattern is improved approximately by 37.3% compared to the conventional walking pattern. Furthermore, the gait synthesis for the real robot SHR-1 and the walking pattern generation for known terrains are clarified in detail. The walking experiments on the flat and slope terrain validate the effectiveness of the proposed pattern generation.

In the future, the more intensive study on the bridge between the active humanoid robot and passive humanoid robot utilizing the PIPM model will be further conducted. In addition, we will also develop the online free pattern generation technology using PIPM with an online control technology to make the biped adapt to unknown terrain and disturbances.

Acknowledgments

This work is partly supported by the Central Academe of Shanghai Electric Group Co., Ltd, the National High Technology Research and Development Program of China under grant 2006AA040203, the Natural Science Foundation of China under grant 60475032 and the Program for New Century Excellent Talents in University.

https://doi.org/10.1017/S0263574710000408 Published online by Cambridge University Press

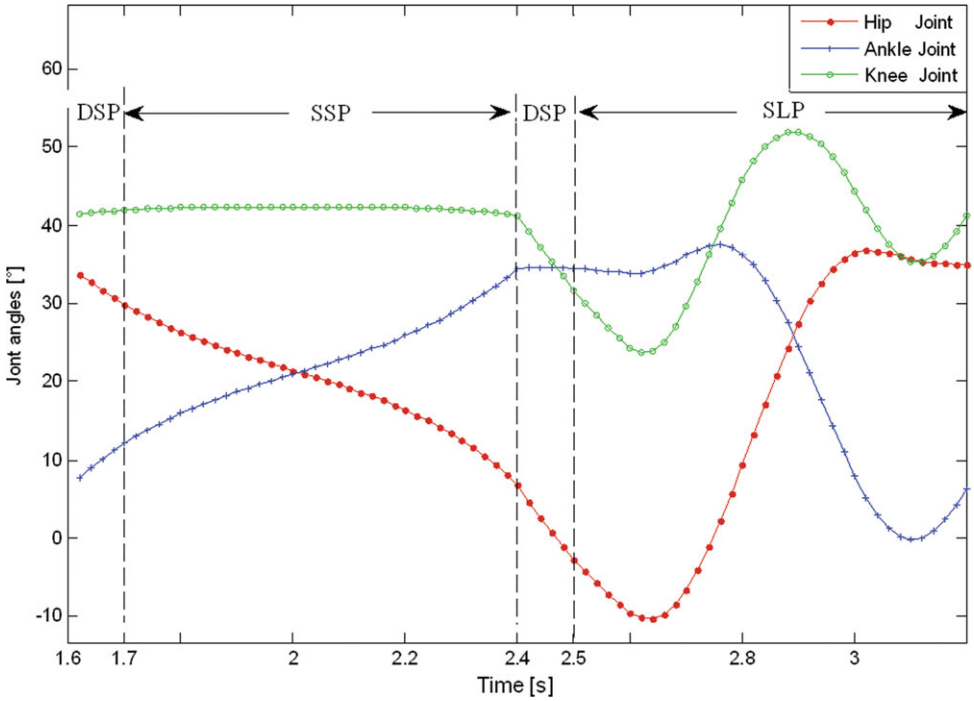

Fig. 8. Angle of joints during one gait period.

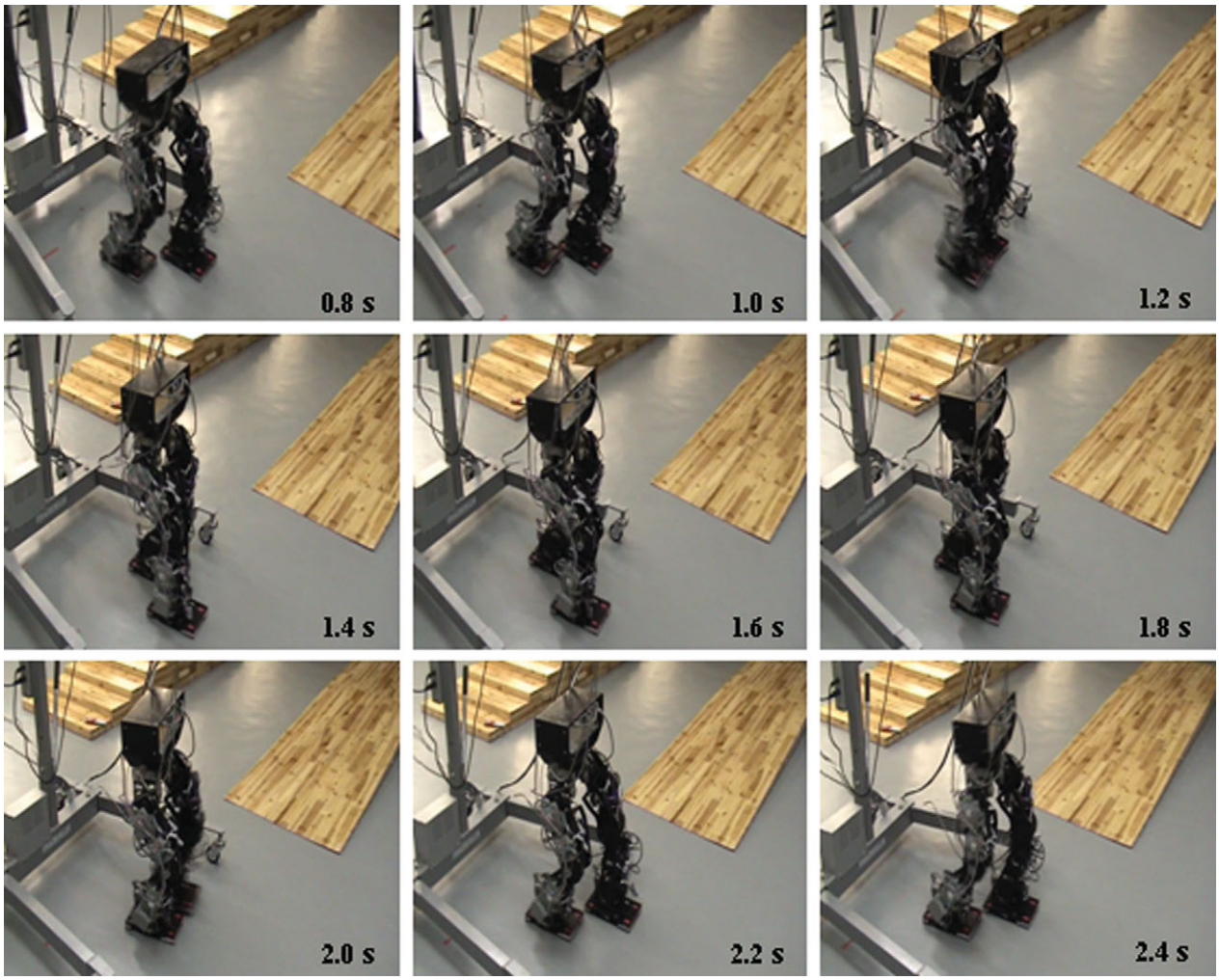

Fig. 9. Snapshots of walking on the flat ground.

https://doi.org/10.1017/S0263574710000408 Published online by Cambridge University Press

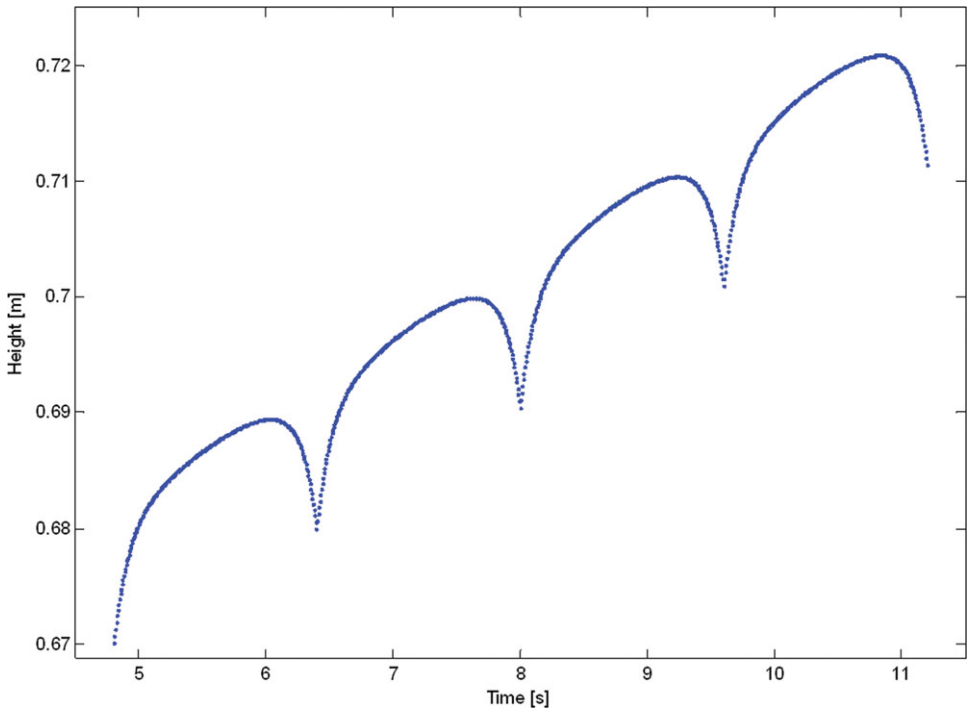

Fig. 10. Height of COG for walking on the slope.

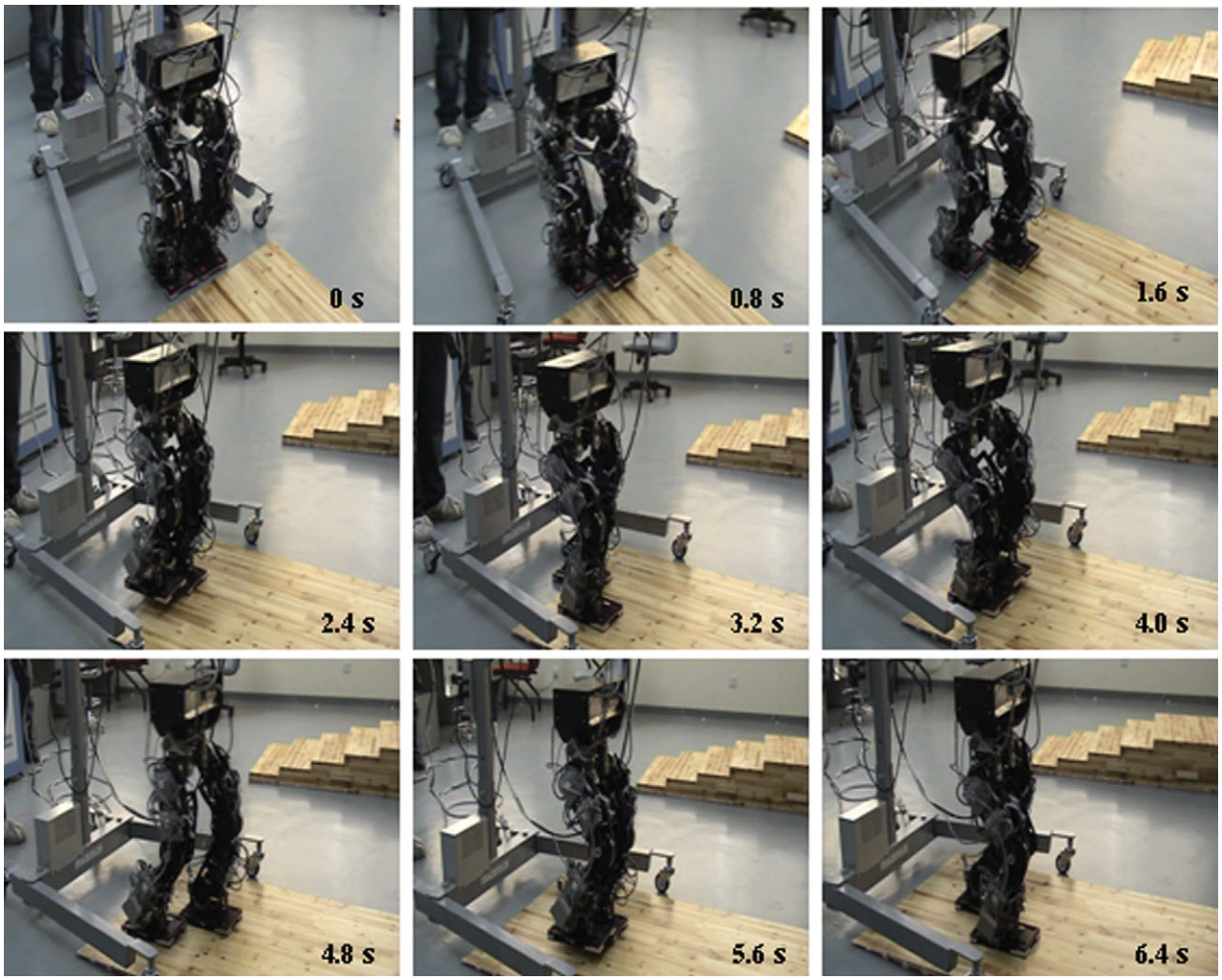

Fig. 11. Snapshots of walking on the slope.

https://doi.org/10.1017/S0263574710000408 Published online by Cambridge University Press

References

1. K. Hirai, M. Hirose, Y. Hacksaw and T. Takeaway, "Development of Honda Humanoid Robot," *Proceedings of the IEEE International Conference on Robotics and Automation*, Leuven, Belgium (1998) pp. 1321–1326.
2. K. Kaneko, F. Kanehiro, S. Kajita, K. Yokoyama, K. Akachi, T. Kawasaki, S. Ota and T. Isozumi, "Design of Prototype Humanoid Robotics Platform for HRP," *Proceedings of the IEEE/RSJ International Conference on Intelligent Robots and Systems*, EPFL, Lausanne, Switzerland (2002) pp. 2431–2436.
3. J. Yamaguchi, S. Inoue, D. Nishino and A. Takanishi, "Development of a Bipedal Humanoid Robot having Antagonistic Driven Joints and Three DOF Trunk," *Proceedings of the IEEE International Conference on Intelligent Robots and Systems*, Victoria, B.C., Canada (1998) pp. 96–101.
4. J. Y. Kim, I. W. Park, J. Lee, M. S. Kim, B. K. Cho and J. H. Oh, "System Design and Dynamic Walking of Humanoid Robot KHR-2," *Proceedings of the IEEE International Conference on Robotics and Automation*, Barcelona, Spain (2005) pp. 1443–1448.
5. M. Gienger, K. Löffler and K. Pfeiffer, "Towards the Design of a Biped Jogging Robot," *Proceedings of the IEEE International Conference on Robotics and Automation*, Seoul, Korea (2001) pp. 4140–4145.
6. M. Vukobratovic, B. Borovac, D. Surla and D. Stokic, *Biped Locomotion: Dynamics, Stability, Control and Application* (Springer Verlag, Berlin, 1990).
7. S. Kajita, F. Kanehiro, K. Kaneko, K. Fujiwara, K. Harada, K. Yokoi and H. Hirukawa, "Biped Walking Pattern Generation by Using Preview Control of Zero-Moment Point," *Proceedings of the IEEE International Conference on Robotics and Automation*, Taipei, Taiwan (2003) pp. 1620–1626.
8. H. Qiang, K. Yokoi, S. Kajita, N. Koyachi, K. Kaneko, H. Arai, K. Komoriya and K. Tanie, "Planning walking patterns for a biped robot," *IEEE Trans. on Robot. Autom.* **17**(3), 280–289 (2001).
9. Z. Tang and M. J. Er, "Humanoid 3D Gait Generation Based on Inverted Pendulum Model," *22nd IEEE International Symposium on Intelligent Control*, Singapore (2007) pp. 339–344.
10. Y. Ogura, H. O. Lim and A. Yakanishi, "Stretch Walking Pattern Generation for a Biped Humanoid Robot," *Proceedings of the IEEE/RSJ International Conference on Intelligent Robots and Systems*, Las Vegas, Nevada (2003) pp. 352–357.
11. Y. Ogura, K. Shimomura, H. Kondo, A. Morishima, T. Okubo, S. Momoki, H. O. Lim and A Takanishi, "Human-like Walking with Knee Stretched, Heel-contact and Toe-off Motion by a Humanoid Robot," *Proceedings of the IEEE/RSJ International Conference on Intelligent and Robots Systems*, Beijing, China (2006) pp. 3976–3981.
12. R. Kurazume, S. Tanaka, M. Yamashita, T. Hasegawa and K. Yoneda, "Straight Legged Walking of a Biped Robot," *Proceedings of the IEEE/RSJ International Conference on Intelligent Robots and Systems*, Fukuoka, Japan (2005) pp. 337–343.
13. A. Sekiguchi, K. Kameta, Y. Tsumaki and D. N. Nenchev, "Biped Walk Based on Vertical Pivot Motion of Linear Inverted Pendulum," *Proceedings of the IEEE/ASME International Conference on Advanced Intelligent Mechatronics*, Zurich, Switzerland (2007) pp. 1–6.
14. T. McGeer, "Passive dynamic walking," *Intern. J. Robot. Res.* **9**(2), 62–82 (1990).
15. T. McGeer, "Stability and control of two-dimensional biped walking," *Technical Report*. CSS-IS TR 88–01, Simon Fraser University, (1988).
16. S. H. Collins, A. Ruina, M. Wisse and R. Tedrake, "Efficient bipedal robots based on passive-dynamic walkers," *Science* **307**, 1082–1085 (2005).
17. S. H. Collins and A. Ruina, "A bipedal Walking Robot with Efficient and Human-like Gait," *Proceedings of the IEEE International Conference Robotics and Automation*, Barcelona, Spain (2005) pp. 1983–1988.
18. S. O. Anderson, M. Wisse, C. G. Atkeson, J. K. Hodgins, G. J. Zeglin and B. Moyer, "Powered Bipeds Based on Passive Dynamic Principles," *IEEE-RAS International Conference on Humanoid Robots*, Tsukuba, Japan (2005) pp. 110–116.
19. F. Asano, M. Yamakita, N. Kamamichi and Z. W. Luo, "A novel gait generation for biped walking robots based on mechanical energy constraint," *IEEE Trans. Robot. Autom.* **20**(3), 565–573 (2004).
20. E. R. Westervelt, J. W. Grizzle and D. E. Koditschek, "Hybrid zero dynamics of planar biped wakers," *IEEE Trans. Robot. Autom.* **48**(1), 42–56 (2003).
21. V. T. Inman, J. J. Ralston and F. Todd, *Human Walking* (Williams & Wilkins, London, UK, 1981).
22. M. Vukobratovich and Y. Ekalo, "Mathematical model of general anthropomorphic systems," *Math. Biosci.* **17**, 191–242 (1973).

https://doi.org/10.1017/S0263574710000408 Published online by Cambridge University Press